NASA TECHNICAL MEMORANDUM

NASA TM X- 64746

SKYLAB ATTITUDE CONTROL AND ANGULAR MOMENTUM DESATURATION WITH ONE DOUBLE-GIMBALED CONTROL MOMENT GYRO

By Hans F. Kennel
Astrionics Laboratory

January 12, 1973

NASA

George C. Marshall Space Flight Center
Marshall Space Flight Center, Alabama

MSFC - Form 3190 (Rev June 1971)

TECHNICAL REPORT STANDARD TITLE PAGE

1. REPORT NO. NASA TM X- 64746	2. GOVERNMENT ACCESSION NO.	3. RECIPIENT'S CATALOG NO.
4. TITLE AND SUBTITLE Skylab Attitude Control and Angular Momentum Desaturation with One Double-Gimbaled Control Moment Gyro		5. REPORT DATE January 12, 1973
		6. PERFORMING ORGANIZATION CODE
7. AUTHOR(S) Hans F. Kennel		8. PERFORMING ORGANIZATION REPORT #
9. PERFORMING ORGANIZATION NAME AND ADDRESS George C. Marshall Space Flight Center Marshall Space Flight Center, Alabama 35812		10. WORK UNIT NO.
		11. CONTRACT OR GRANT NO.
		13. TYPE OF REPORT & PERIOD COVERED Technical Memorandum
12. SPONSORING AGENCY NAME AND ADDRESS National Aeronautics and Space Administration Washington, D.C. 25046		
		14. SPONSORING AGENCY CODE

15. SUPPLEMENTARY NOTES

Prepared by Astrionics Laboratory, Science and Engineering

16. ABSTRACT In case two control moment gyros fail, attitude control of Skylab can be maintained with the thruster attitude control system. This results, however, in a severely increased fuel consumption, depleting the fuel in a few days. A reduction in fuel consumption can be achieved by allowing the attitude reference to yield with the gravity-gradient torques at twice orbital frequency. For an ideal case, fuel consumption can be drastically reduced, but any unanticipated disturbance torques and principal moment-of-inertia axes misalignments will again increase the fuel consumption sizeably. Therefore, an alternate concept was developed, which does not have large fuel consumption under any circumstances. In this concept the attitude reference is commanded to oscillate in the orbital plane with twice the orbital frequency and the remaining control moment gyro controls about orbital north and about the minimum moment-of-inertia axis, while the thruster attitude control system controls rate only about the remaining axis. This rate control in conjunction with the restoring torque due to the gravity gradient will keep bounded the excursion of the minimum moment-of-inertia axis out of the orbital plane. This alternate concept has the additional advantage that it needs no information on the principal moment-of-inertia axes misalignment and is completely insensitive to star tracker failure. Proper phasing of the attitude reference oscillation even allows angular momentum desaturation, which is responsible for the insensitivity of the thruster fuel consumption to unknown disturbances, like vent torques, magnetic torques, etc.

17. KEY WORDS Space Station, Control Moment Gyros, Angular Momentum Desaturation, Control Law Gravity Torque	18. DISTRIBUTION STATEMENT Unclassified-unlimited Hans F. Kennel

19. SECURITY CLASSIF. (of this report)	20. SECURITY CLASSIF. (of this page)	21. NO. OF PAGES	22. PRICE
Unclassified	Unclassified	52	NTIS

MSFC - Form 3292 (Rev December 1972) For sale by National Technical Information Service, Springfield, Virginia 22151

TABLE OF CONTENTS

LIST OF ILLUSTRATIONS

LIST OF TABLES

LIST OF SYMBOLS

Symbol	Definition
A	[rad] amplitude of commanded y-oscillation
c	cosine (with Greek symbol)
e_{ij}	CMG direction cosines in CS X_v ($i = 1, 2, 3; j = 1, 2, 3$)
$\dot{e}_{ci}$	[1/s] normalized torque command ($i = 1, 2, 3$)
f_t	[N] cold gas thruster force
G_{yd}	[N·m·s/rad] desaturation angle effectiveness
H	[N·m·s] CMG momentum magnitude
H_{cyc}	[N·m·s] amplitude of cyclic momentum
H_{max}	[N·m·s] maximum of H_{yo}
H_{min}	[N·m·s] minimum of H_{yo}
H'_{max}	[N·m·s] adjusted maximum of H_{yo}
H'_{min}	[N·m·s] adjusted minimum of H_{yo}
H_p	[N·m·s] average peak momentum
H_{pp}	[N·m·s] allowable peak-to-peak momentum
H_r	[N·m·s] ramp momentum
H_{xo}, H_{yo}	[N·m·s] CMG momentum components in CS X_{or}
H_{xv}, H_{yv}	[N·m·s] CMG momentum components in CS X_v
H_{zo}	[N·m·s] vehicle orbital z-momentum
H_{xb}	[N·m·s] nominal CMG x-momentum in CS X_v
H_{xll}, H_{xul}	[N·m·s] lower and upper limit imposed on H_{xv}

LIST OF SYMBOLS (Continued)

Symbol	Definition
H_{yl}	[N·m·s] limit imposed on $\lvert H_{yo} \rvert$
H_{yll}, H_{yul}	[N·m·s] lower and upper values of $\lvert H_{yo} \rvert$ used for TACS firing decisions
$H'_{yo(n-1)}$	[N·m·s] adjusted H_{yo} value of last checkpoint
I	[kg·m^2] representative moment of inertia
I_x, I_y, I_z	[kg·m^2] principal moments of inertia
I_{TACS}	[N·s] total TACS impulse
I_1, I_2	integrals
K_c	$= 2Ac2\phi_{yd}$
K_d	weighing factor
K_p	weighing factor
K_{pp}	weighing factor
K_r	factor used for peak adjustment
K_s	$= 2As2\phi_{yd}$
K_{yd}	$= -1/G_{yd}$
K_Δ	[N·m·s/rad] effectiveness of $\Delta\phi_{yd}$ on H_{yo}
K_ϕ	effectiveness of phase shift due to ΔH_r on ΔH_p
q_{vai}	quaternion (CS X_r to CS X_v) ($i = 1, 2, 3, 4$)
r_x, r_y, r_z	direction cosines of gravity gradient in CS X_v
R_x	[m] thruster lever arm along x_v (negative)

LIST OF SYMBOLS (Continued)

Symbol	Definition
s	sine (with Greek symbol)
t	[s] monotonically increasing time base
$\underline{T}_{gg}$	[N· m] gravity-gradient torque (CS X_v components)
$\underline{T}_{ggo}$	[N· m] gravity-gradient torque (CS X_{or} components)
T_{xo}, T_{yo}, T_{zo}	[N· m] components of $\underline{T}_{ggo}$
t_{max}, t_{min}	[s] time of occurrence of H_{max}, H_{min}
t_{td}	[s] thrust decay correction
α	[rad] dummy integration variable
$\delta_{1(i)}$	[rad] inner gimbal angle of CMG # i
$\delta_{3(i)}$	[rad] outer gimbal angle of CMG # i
ΔH	[N· m· s] negative y- or z-momentum change for one MIB
$\Delta H'$	[N· m· s] nominal z-momentum change for one MIB
ΔH_p	[N· m· s] peak momentum off-set
ΔH_r	[N· m· s] momentum ramp
ΔH_x	[N· m· s] negative x-momentum change for one MIB
ΔH_{yo}	[N· m· s] orbital y-momentum change for TACS firing
ΔH_{zo}	[N· m· s] orbital z-momentum change for TACS firing
$(\Delta H)_{\Delta\phi_{yd}}$	[N· m· s] momentum change due to $\Delta\phi_{yd}$

LIST OF SYMBOLS (Continued)

Symbol	Definition
ΔI	[$kg \cdot m^2$] representative moment-of-inertia difference
Δt_{mib}	[s] nominal MIB on-time
$\Delta \dot{\phi}_{yc}$	[rad/s] change in $\dot{\phi}_{yc}$
$\Delta \phi_{yd}$	[rad] change in ϕ_{yd}
$(\Delta \phi_{yd})_p$	[rad] portion of $\Delta \phi_{yd}$ due to peak off-set
$(\Delta \phi_{yd})_r$	[rad] portion of $\Delta \phi_{yd}$ due to ramp momentum
$\Delta \phi_{ydl}$	[rad] limit imposed on $\Delta \phi_{yd}$
ϵ_i, $\dot{\epsilon}_i$	[rad, rad/s] attitude error and rate commands $(i = x, y, z)$
η_t	[rad] see Appendix A for definition
η_{tt}	[rad] $= \eta_t - \phi_{yc}$
η_x	[rad] see Appendix A for definition
η_y	[rad] see Appendix A for definition
$\sum \Delta H_{yoy}$	[$N \cdot m \cdot s$] accumulated ΔH_{yo} due to y-firings
$\sum \Delta H_{yoz}$	[$N \cdot m \cdot s$] accumulated ΔH_{yo} due to z-firings
$\dot{\phi}_i$	[rad/s] vehicle angular velocity in CS X_v $(i = x, y, z)$
ϕ_{ie}, $\dot{\phi}_{ie}$	[rad, rad/s] attitude and rate errors in CS X_v $(i = x, y, z)$
ϕ_{ieo}, $\dot{\phi}_{ieo}$	[rad, rad/s] attitude and rate errors in CS X_{or} $(i = x, y, z)$
ϕ_{yb}	[rad] y bias angle

LIST OF SYMBOLS (Concluded)

Symbol	Definition
ϕ_{yc}, $\dot{\phi}_{yc}$	[rad, rad/s] commanded orbital y-angle and its rate
ϕ_{yd}	[rad] orbital y-desaturation angle
ϕ_{ydl}	[rad] upper limit imposed on $\lvert\phi_{yd}\rvert$
ϕ_{ydll}	[rad] lowest allowable value for ϕ_{ydl}
ψ_i	TACS firing indicators (i = x, y, z)
ψ_{io}	TACS firing indicators (i = x, y, z)
ω_{ij}	[rad/s] CMG angular velocity commands (i = 1, 2, 3; j = 1, 2, 3)
Ω	[rad/s] orbital angular velocity

$$[\beta_x] = \begin{bmatrix} 1 & 0 & 0 \\ 0 & c\beta_x & s\beta_x \\ 0 & -s\beta_x & c\beta_x \end{bmatrix}$$

$$[\beta_y] = \begin{bmatrix} c\beta_y & 0 & -s\beta_y \\ 0 & 1 & 0 \\ s\beta_y & 0 & c\beta_y \end{bmatrix}$$

$$[\beta_z] = \begin{bmatrix} c\beta_z & s\beta_z & 0 \\ -s\beta_z & c\beta_z & 0 \\ 0 & 0 & 1 \end{bmatrix}$$

where β can be any Greek symbol

TECHNICAL MEMORANDUM X- 64746

SKYLAB ATTITUDE CONTROL AND ANGULAR MOMENTUM DESATURATION WITH ONE DOUBLE-GIMBALED CONTROL MOMENT GYRO

INTRODUCTION

The Skylab is a scientific space station in circular earth orbit with more or less cylindrical moment-of-inertia distribution. The minimum moment-of-inertia axis is nominally in the orbital plane and perpendicular to the sunline. The attitude is normally maintained by three double-gimbaled control moment gyros (CMG) [1]. Several possibilities exist on how to control the attitude when two CMG's have failed and normal attitude control and angular momentum desaturation [2, 3] have to be abandoned. The possible attitude control concepts are the following:

<u>Concept A.</u> The nominal attitude reference is retained; the remaining CMG is also deactivated and the thruster attitude control system (TACS) controls all axes to the specified attitude and rate deadbands.

<u>Concept B.</u> The nominal attitude reference is retained; the remaining CMG controls sun-pointing (two axes) accurately and the TACS controls the third axis within a specified attitude and rate deadband.

<u>Concept C.</u> The attitude reference follows an unstable limit cycle of about 0.3 rad amplitude which the vehicle exhibits if it is allowed to yield under the influence of gravity-gradient torques; the remaining CMG is also deactivated and the TACS controls all axes to the specified attitude and rate deadbands.

<u>Concept D.</u> The attitude reference is commanded to oscillate in the orbital plane with 0.2 rad amplitude and twice orbital frequency; the remaining CMG controls the commanded attitude about orbital north accurately as well as the attitude about the vehicle minimum principal moment-of-inertia axis and the TACS controls about the projection of the sunline into the orbital plane, but to a rate deadband only.

The advantages and disadvantages of the concepts are discussed in the following paragraphs. The numerical values are based on the vehicle data of Tables 1, 2, and 3.

TABLE 1. GENERAL DATA

CMG Momentum Magnitude	$H = 3115.3$ [N·m·s]
TACS Minimum Impulse Bit	MIB = 18 [N·s]
Momentum Change in x for one MIB	$\Delta H_x = 60$ [N·m·s]
Momentum Change in y or z for one MIB	$\Delta H = 210$ [N·m·s]
Total TACS Fuel Available (in Impulse Units)	$I_{tacs} = 160\ 000$ [N·s]

TABLE 2. COMMAND/SERVICE MODULE DOCKED TO SKYLAB

Minimum Moment-of-Inertia	$I_x = 0.992 \cdot 10^6$ [kg·m²]
Intermediate Moment-of-Inertia	$I_z = 6.168 \cdot 10^6$ [kg·m²]
Maximum Moment-of-Inertia	$I_y = 6.245 \cdot 10^6$ [kg·m²]
Amplitude of Cyclic Momentum (Concepts A and B)	$H_{cyc} \approx 4500$ [N·m·s]

TABLE 3. COMMAND/SERVICE MODULE NOT DOCKED TO SKYLAB

Minimum Moment-of-Inertia	$I_x = 0.893 \cdot 10^6$ [kg·m²]
Intermediate Moment-of-Inertia	$I_y = 3.813 \cdot 10^6$ [kg·m²]
Maximum Moment-of-Inertia	$I_z = 3.882 \cdot 10^6$ [kg·m²]
Amplitude of Cyclic Momentum (Concepts A and B)	$H_{cyc} \approx 2800$ [N·m·s]

Concepts A and B require no modification of the attitude error generation. However, the cyclic angular momentum caused by the gravity-gradient torque is so large that the available TACS fuel is exhausted within 3 days (assuming 50 000 [N·s] available at the beginning) for Concept A and within about 5 days for Concept B; i.e., the mission would have to be terminated very soon. Concept A would not allow many solar experiments, whereas Concept B would allow most. Concept C has been called quasi-inertial attitude control [4,5] and for an ideal case the fuel consumption has been reduced drastically. The fuel consumption is unfortunately very sensitive to the knowledge of the principal moment-of-inertia axes misalignment and to the knowledge of the attitude of the minimum principal moment-of-inertia axis with respect to the orbital plane (requiring a functioning star tracker) and increases with the addition of other disturbance torques besides the gravity-gradient torque. Only the biomedical experiments can be performed for Concepts C and D. The fuel consumption for Concept D, however, can be made completely insensitive to information on principal moment-of-inertia axes misalignment, and disturbance torques and does not require star tracker information since no attitude information is used for the TACS command, but only rate information. The worst case fuel consumption can be held below 50 [N·s] per orbit for all solar elevation angles with respect to the orbital plane and all projected disturbance torques. The control system parameters, however, are assumed to be reasonably close to their optimum. This compares very favorably with the 100 [N·s] per orbit for Concept C, and the 1200 [N·s] per orbit for Concept A. It should be pointed out again that the low fuel consumption for Concept C only applies to the ideal case where the principal moment-of-inertia axes misalignments are known exactly and where there are no disturbance torques other than the gravity gradient torque. A 50 [N·s] per orbit figure is equivalent to 66 days operation (assuming 50 000 [N·s] TACS fuel available at the beginning) versus less than 3 days operation for 1200 [N·s] per orbit. The attitude reference oscillation is required for Concept D so that part of the cyclic momentum is stored in the vehicle, reducing the remainder to the point where one CMG can accommodate it and have some margin for control. The details of Concept D are set forth in the body of this report.

GRAVITY-GRADIENT TORQUES AND ACCUMULATED MOMENTUM

When the gravity-gradient torque is expressed about vehicle principal axis, one has [3]

$$\underline{T}_{gg} = 3\Omega^2 \begin{bmatrix} (I_z - I_y) r_y r_z \\ (I_x - I_z) r_z r_x \\ (I_y - I_x) r_x r_y \end{bmatrix} \tag{1}$$

where it is assumed that the space vehicle is in a circular orbit with angular velocity Ω ; I_x, I_y, I_z are principal moments of inertia; and r_x, r_y, r_z are the components of the local vertical in the principal coordinate system.

To bring out the essentials of single CMG control for Skylab, it can be assumed that there is no misalignment between geometric and principal axes and that $I_y = I_z = I$ or $\Delta I = I_y - I_x = -(I_x - I_z)$ which also allows one to disregard the solar elevation angle η_x (see Appendix A for definition) since now any two mutually perpendicular axes, which are also perpendicular to the principal x-axis, are principal axes. With this simplification, one has

$$\underline{T}_{gg} = 3\Omega^2 \Delta I r_x \begin{bmatrix} 0 \\ -r_z \\ r_y \end{bmatrix} . \tag{2}$$

Now, one assumes that the vehicle is rigidly controlled about orbital y to the angle ϕ_{yc} and about vehicle x to zero, while it is allowed to have a small error ϕ_{zeo} in orbital z. Then, one has

$$\begin{bmatrix} r_x \\ r_y \\ r_z \end{bmatrix} = \begin{bmatrix} 1 & \phi_{zeo} & 0 \\ -\phi_{zeo} & 1 & 0 \\ 0 & 0 & 1 \end{bmatrix} \begin{bmatrix} c\eta_{tt} & 0 & s\eta_{tt} \\ 0 & 1 & 0 \\ -s\eta_{tt} & 0 & c\eta_{tt} \end{bmatrix} \begin{bmatrix} 0 \\ 0 \\ -1 \end{bmatrix} = \begin{bmatrix} -s\eta_{tt} \\ +\phi_{zeo} s\eta_{tt} \\ -c\eta_{tt} \end{bmatrix} \tag{3}$$

where $\eta_{tt} = \eta_t - \phi_{yc}$ and η_t is the angle from orbital midnight. Small angle approximations have been assumed for ϕ_{zeo} with $c\phi_{zeo} = 1$ and $s\phi_{zeo} = \phi_{zeo}$. Insertion of the r components into equation (2) yields

$$\underline{T}_{gg} = -3\Omega^2 \Delta I \begin{bmatrix} 0 \\ s\eta_{tt}\, c\eta_{tt} \\ \phi_{zeo}\, s^2\eta_{tt} \end{bmatrix} .$$

Transformation into orbital coordinates and substitution of $(\eta_t - \phi_{yc})$ for η_{tt} yields

$$\underline{T}_{ggo} = -3\Omega^2 \Delta I \begin{bmatrix} c\phi_{yc} & 0 & s\phi_{yc} \\ 0 & 1 & 0 \\ -s\phi_{yc} & 0 & c\phi_{yc} \end{bmatrix} \begin{bmatrix} 1 & -\phi_{zeo} & 0 \\ \phi_{zeo} & 1 & 0 \\ 0 & 0 & 1 \end{bmatrix} \begin{bmatrix} 0 \\ s2(\eta_t - \phi_{yc})/2 \\ \phi_{zeo} s^2(\eta_t - \phi_{yc}) \end{bmatrix}$$

$$= -\frac{3}{2}\Omega^2 \Delta I \begin{bmatrix} 2\phi_{zeo} s(\eta_t - \phi_{yc}) c\eta_t \\ s2(\eta_t - \phi_{yc}) \\ 2\phi_{zeo} s(\eta_t - \phi_{yc}) s\eta_t \end{bmatrix} . \qquad (4)$$

The orbital y-torque will be discussed first, since it is not a function of the small angle ϕ_{zeo}. The angle ϕ_{yc} allows the vehicle to yield some under the influence of the gravity-gradient torques and, therefore, absorb angular momentum which otherwise would saturate the one operative CMG. The following form is chosen for the orbital y-command (A is a constant amplitude)

$$\phi_{yc} = As2(\eta_t - \phi_{yd})$$

which yields for the orbital y-torque [refer to equation (4)]

$$T_{yo} = -\frac{3}{2}\Omega^2 \Delta Is2[\eta_t - As2(\eta_t - \phi_{yd})] \quad .$$

The angle ϕ_{yd} is a desaturation angle. This is shown in Appendix B with the results that the momentum accumulated over half an orbit is (H_{yoic} is the initial condition)

$$H_{yo} - H_{yoic} = -6\Omega\Delta I \int_0^{\pi/4} c2\eta_t c(K_c s2\eta_t) s(K_s c2\eta_t) d\eta_t \tag{5}$$

with $K_c = 2Ac2\phi_{yd}$ and $K_s = 2As2\phi_{yd}$. The actual integration in equation (5) is only from 0 to $\pi/4$ due to utilization of symmetry properties (see Appendix B). $H_{yo}(\eta_t)$ for three different values of ϕ_{yd} is shown in Figure 1. When ϕ_{yd} is small, equation (5) simplifies to

$$H_{yo} - H_{yoic} = G_{yd}\phi_{yd} \tag{6}$$

with $G_{yd} = -24\Omega\Delta I\, A \int_0^{\pi/4} c^2(2\eta_t)c(2As2\eta_t)d\eta_t$. Equation (6) shows that the accumulated momentum is proportional to ϕ_{yd}, and the desaturation angle effectiveness G_{yd} is roughly proportional to the amplitude A.

The orbital z-torque of equation (4) is

$$T_{zo} = -\{3\Omega^2\Delta Is[\eta_t - As2(\eta_t - \phi_{yd})]s\eta_t\}\phi_{zeo} \quad .$$

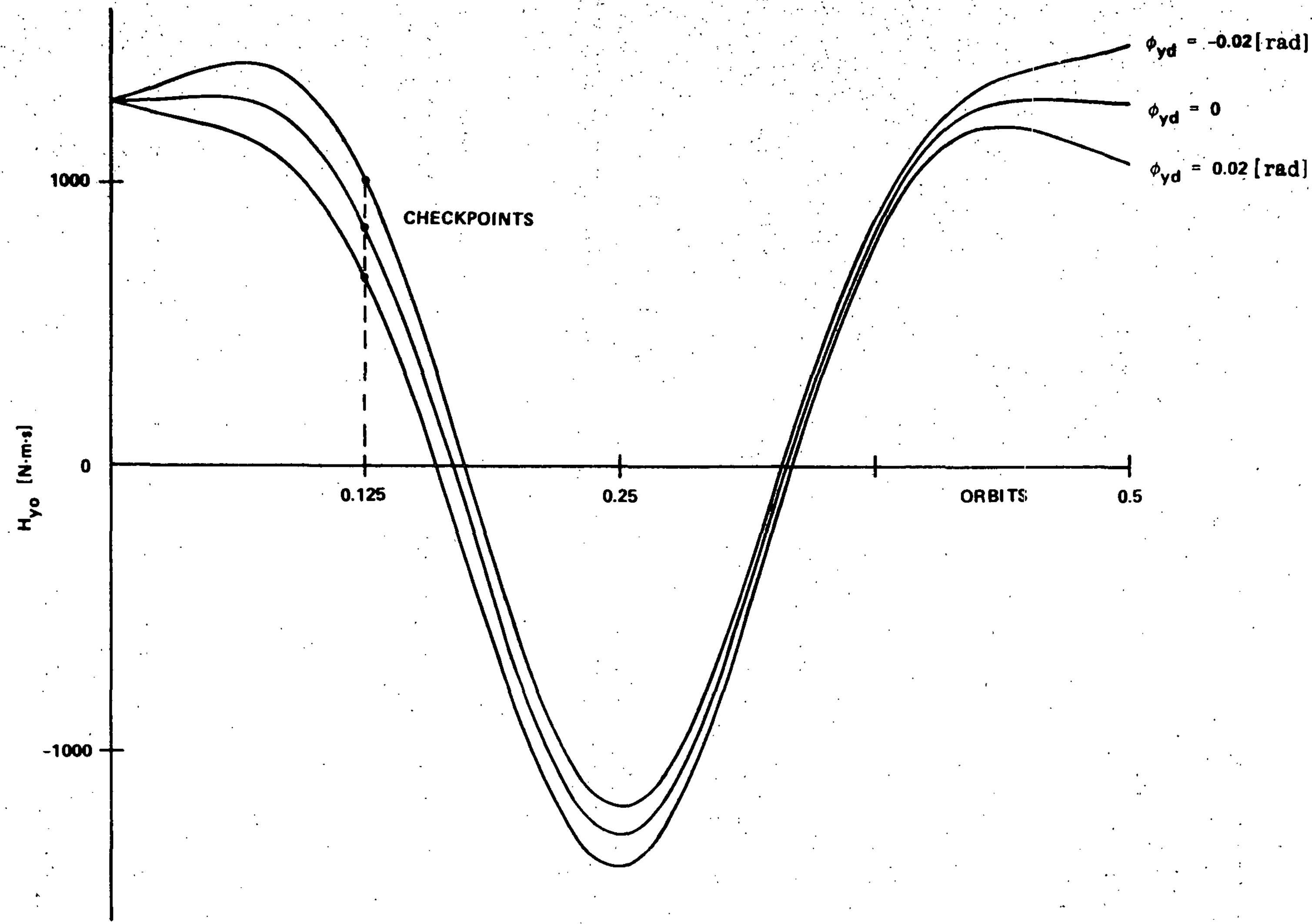

Figure 1. CMG orbital y-momentum component (ideal limit cycle).

This torque has in general the opposite sign of ϕ_{zeo}. Only very temporarily (for $\phi_{yd} \neq 0$ and η_t small) can it have the same sign as ϕ_{zeo}. It is, therefore, a restoring torque which drives the minimum principal moment-of-inertia axis toward the orbital plane. However, since the quantity in braces is not a constant, instability occurs unless damping is provided. Nonlinear damping is provided by the fact that thrusters are fired to reduce $\dot{\phi}_{zeo}$ whenever it exceeds a specific deadband. The result is that the angular excursions of ϕ_{zeo} are kept within acceptable limits.

The orbital x torque of equation (4) is

$$T_{xo} = -\{3\Omega^2 \Delta I \, s(\eta_t - \phi_{yc}) c\eta_t\}\phi_{zeo} \quad .$$

Since ϕ_{zeo} is not directly controlled, no control is possible over the accumulated x momentum. It has to be absorbed by the CMG and thruster firings will keep the momentum within acceptable limits.

ORBITAL y-MOMENTUM DESATURATION

The commanded orbital oscillation ϕ_{yc} must be exactly in phase with the direction of the gravity gradient, or bias momentum accumulates as shown in the section on Gravity-Gradient Torques and Accumulated Momentum. On the other hand, this fact can be used to desaturate orbital y-momentum, as well as seek the direction of the principal x-axis. The commanded oscillation is

$$\phi_{yc} = As2(\eta_t - \phi_{yd}) \tag{7}$$

where ϕ_{yd} is a desaturation angle to be updated every half orbit. Any change of ϕ_{yd} will also lead to a change in ϕ_{yc}. This causes a maneuver requiring momentum from the CMG. The start of the maneuver, i.e., the checkpoint, should be placed at a point when ample momentum is available, i.e., away from the momentum peaks. The times when $\eta_t = \pi/4$ and $\eta_t = 5\pi/4$ have been selected as the two checkpoints per orbit. A typical momentum curve (docked configuration) for no inertia misalignment and no other than gravity-gradient torques is shown in Figure 1.

In general, a momentum ramp ΔH_r will be superimposed on the cyclic momentum. The basic desire for the desaturation angle change $\Delta\phi_{yd}$ is to eliminate the ramp and simultaneously average the momentum peaks:

$$\begin{aligned}\Delta\phi_{yd} &= (\Delta\phi_{yd})_p + (\Delta\phi_{yd})_r \\ &= K_{yd}(\Delta H_p + \Delta H_r)\end{aligned}$$

with $K_{yd} = -1/G_{yd}$. While the steady-state effect of ϕ_{yd} is given by equation (6), a $\Delta\phi_{yd}$ also has other effects. One is the different momentum stored in the vehicle due to the difference in $\dot{\phi}_{yc}$:

$$\begin{aligned}\Delta\dot{\phi}_{yc} &= \dot{\phi}_{yc}(+) - \dot{\phi}_{yc}(-) \\ &= 2\Omega A c2[\eta_t - (\phi_{yd} + \Delta\phi_{yd})] - 2\Omega A c2[\eta_t - \phi_{yd}] \quad . \qquad (8)\end{aligned}$$

For sufficiently small $\Delta\phi_{yd}$ ($c2\Delta\phi_{yd} \approx 1$, $s2\Delta\phi_{yd} \approx 2\Delta\phi_{yd}$), one has

$$\begin{aligned}\Delta\dot{\phi}_{yc} &\approx -4\Omega A s2(\eta_t - \phi_{yd})\Delta\phi_{yd} \\ &\approx -4\Omega\, \phi_{yc}\Delta\phi_{yd}\end{aligned}$$

or

$$(\Delta H)_{\Delta\phi_{yd}} = K_\Delta \Delta\phi_{yd}$$

with $K_\Delta = -4\Omega I \phi_{yc}$. The existing ramp can be established by

$$\Delta H_r = H_{yo} - H'_{yo(n-1)} \tag{9}$$

with $H'_{yo(n-1)} = H_{yo(n-1)} + K_{\Delta(n-1)} \Delta\phi_{yd(n-1)}$, where the (n-1) indicates the values at the last checkpoint. To average the peaks, one uses

$$\Delta H_p = (H_{max} + H_{min})/2 + (\partial H_p/\partial H_r)\Delta H_r \quad . \tag{10}$$

The effect of ΔH_r on the peaks can be broken down into three different parts:

$$(\partial H_p/\partial H_r) = K_r + K_\Delta K_{yd} + K_\phi \quad .$$

Looking back, the peaks should be adjusted to

$$H'_{max} = H_{max} + [(t-t_{max})/(0.5T_{orb})]\Delta H_r$$

$$H'_{min} = H_{min} + [(t-t_{min})/(0.5T_{orb})]\Delta H_r \quad .$$

Both effects can be combined into $K_r \Delta H_r$ with

$$K_r = (2t-t_{max}-t_{min})/T_{orb} \quad . \tag{11}$$

Looking ahead, the elimination of the ramp will generate a momentum change of $K_\Delta K_{yd} \Delta H_r$ and will affect the peaks some more by the phase shift and by the change of form of the momentum curve. These effects are lumped into $K_\phi \Delta H_r$. Since the value of K_ϕ depends on the angle ϕ_{yd}, on the vent torques, and on the value of the ramp, an acceptable K_ϕ has to be established by simulation.

The final result is

$$\Delta\phi_{yd} = K_{yd}\{(H_{max}+H_{min})/2 + (1+K_r+K_\Delta K_{yd}+K_\phi)(H_{yo}-H'_{yo(n-1)})\} . \tag{12}$$

To avoid excessive maneuver momentum requirements or maneuver time, $\Delta\phi_{yd}$ is limited to $\Delta\phi_{ydl}$. The larger the nongravitational disturbance torque, the larger the desaturation angle and the larger the peak-to-peak distance of the cyclic component of the orbital y-momentum. But the peak-to-peak distance $(H_{max}-H_{min})$ has to be kept below twice the orbital y-momentum limit to avoid TACS firings which do not oppose the disturbance torques. This can be achieved by a limit placed on ϕ_{yd}. The value of the limit cannot be a constant, since it depends on the inertia misalignment and, also, on the disturbance torque level. Therefore, the value of the limit has to be changed, when the changing conditions demand it. When the peak-to-peak distance is below its allowed maximum H_{pp} and the desaturation angle ϕ_{yd} was not on the limit for the past half orbit, no adjustment of the limit ϕ_{ydl} is necessary. If, however, ϕ_{yd} was on its limit, the limiting value is too low and has to be increased. If the peak-to-peak distance is more than H_{pp}, the limiting value has to be decreased, whether ϕ_{yd} was limited or not. A minimum value is also imposed on the limit itself, since its lowest reasonable value can easily be established, but transients could let the limit drop lower.

After ϕ_{yd} is updated by $\Delta\phi_{yd}$, it is limited to the latest value of ϕ_{ydl}. Details of the logic and equations are given in Appendix C.

ATTITUDE ERROR GENERATION AND CMG CONTROL LAW

A double-gimbaled CMG with fixed angular momentum magnitude H has only two degrees of freedom and, therefore, can control only two axes. It was decided to select the vehicle geometric reference axis x_v and the orbital north axis y_{or} (see Appendix A for coordinate system definitions). Several other x-axis choices could have been made (x_{pr}, x_{or}) but these would have resulted in more complex equations and would have required additional information and angles (moment-of-inertia misalignment, principal z_p-axis elevation). The orbital north axis is determined under the assumption that the vehicle x_v-axis is in the orbital plane. The resulting error is small and can be tolerated. Otherwise, accurate angle information about the sunline would be necessary, requiring the star tracker to be operative.

The commanded oscillation about the orbital north is achieved by generation of the attitude error and rate error as

$$\begin{bmatrix} \phi_{xe} \\ \phi_{ye} \\ \phi_{ze} \end{bmatrix} = 2\,\mathrm{sgn}(q_{va4}) \begin{bmatrix} q_{va1} \\ q_{va2} \\ q_{va3} \end{bmatrix} - \begin{bmatrix} 0 \\ \epsilon_y \\ \epsilon_z \end{bmatrix} \tag{13}$$

$$\begin{bmatrix} \dot{\phi}_{xe} \\ \dot{\phi}_{ye} \\ \dot{\phi}_{ze} \end{bmatrix} = \begin{bmatrix} \dot{\phi}_x \\ \dot{\phi}_y \\ \dot{\phi}_z \end{bmatrix} - \begin{bmatrix} 0 \\ \dot{\epsilon}_y \\ \dot{\epsilon}_z \end{bmatrix} \tag{14}$$

with

$$\epsilon_y = \phi_{yc} c\eta_x$$

$$\epsilon_z = -\phi_{yc} s\eta_x$$

$$\dot{\epsilon}_y = \dot{\phi}_{yc} c\eta_x$$

$$\dot{\epsilon}_z = -\dot{\phi}_{yc} s\eta_x$$

and

$$\phi_{yc} = As2(\eta_t - \phi_{yd}) \tag{15}$$

$$\dot{\phi}_{yc} = 2\Omega Ac2(\eta_t - \phi_{yd}) \tag{16}$$

where q_{vai} $(i = 1, 2, 3, 4)$ are quaternions relating CS X_v to CS X_r, A is the amplitude of the commanded oscillation ϕ_{yc}, Ω is the average orbital rate, and ϕ_{yd} is an orbital y-momentum desaturation angle (see chapter on desaturation).

The attitude and rate errors have to be modified as follows:

$$\begin{bmatrix} \phi_{xeo} \\ \phi_{yeo} \\ \phi_{zeo} \end{bmatrix} = [\eta_x]^T \begin{bmatrix} \phi_{xe} \\ \phi_{ye} \\ \phi_{ze} \end{bmatrix} \tag{17}$$

$$\begin{bmatrix} \dot{\phi}_{xeo} \\ \dot{\phi}_{yeo} \\ \dot{\phi}_{zeo} \end{bmatrix} = [\eta_x]^T \begin{bmatrix} \dot{\phi}_{xe} \\ \dot{\phi}_{ye} \\ \dot{\phi}_{ze} \end{bmatrix} \qquad (18)$$

$$\begin{bmatrix} \phi'_{xe} \\ \phi'_{ye} \\ \phi'_{ze} \end{bmatrix} = [\eta_x] \begin{bmatrix} \phi_{xeo} \\ \phi_{yeo} \\ 0 \end{bmatrix} \qquad (19)$$

$$\begin{bmatrix} \dot{\phi}'_{xe} \\ \dot{\phi}'_{ye} \\ \dot{\phi}'_{ze} \end{bmatrix} = [\eta_x] \begin{bmatrix} \dot{\phi}_{xeo} \\ \dot{\phi}_{yeo} \\ 0 \end{bmatrix} \qquad (20)$$

The orbital z-component in $\underline{\phi}_e$ and $\underline{\dot{\phi}}_e$ have been suppressed. The attitude error can now be limited to a relatively small value, without the possibility that a possibly large orbital z-error becomes bothersome (would limit the commandable velocity when $\eta_x \neq 0$).

The normalized CMG torque command can now be generated as usual [5].

$$\dot{e}_{c1} = K_{ox}\phi'_{xe} + K_{1x}\dot{\phi}'_{xr} \qquad (21)$$

$$\dot{e}_{c2} = K_{oy}\phi'_{ye} + K_{1y}\dot{\phi}'_{ye} \qquad (22)$$

$$\dot{e}_{c3} = K_{oz}\phi'_{ze} + K_{1z}\dot{\phi}'_{ze} \qquad . \tag{23}$$

(The normally applied bending filter is neglected here.)

A CMG steering law of the form

$$\begin{bmatrix} \omega_{i1} \\ \omega_{i2} \\ \omega_{i3} \end{bmatrix} = \begin{bmatrix} e_{i1} \\ e_{i2} \\ e_{i3} \end{bmatrix} \times \begin{bmatrix} \dot{e}_{c1} \\ \dot{e}_{c2} \\ e_{c3} \end{bmatrix} \qquad i = 1, 2, 3 \tag{24}$$

(known as the cross-product steering law) will provide a torque component in the desired direction, but its magnitude will always be smaller than desired. This gain reduction can be ignored because the gain drops only to 70 percent (TACS firings prevent lower values) for the worst case orbital desaturation transient and is normally higher than 95 percent. While the CMG will provide x- and y-control, the necessary change of its z-momentum component will act as a disturbance on the z-axis.

The cyclic orbital y-momentum and the commanded oscillation about orbital y (it results in an oscillation of the CMG angular momentum vector in vehicle space) can be accommodated by a "window" of about $\pm\pi/12$ width in the orbital plane and about $\pm\pi/4$ height along orbital north. This window is enforced through TACS firings (see TACS control). The center of the window has been selected as follows: (for $\eta_x = 0$)

<u>For CMG No. 1 operative</u>

$$\begin{bmatrix} e_{11} \\ e_{12} \\ e_{13} \end{bmatrix} = \begin{bmatrix} +0.479 \\ 0 \\ -0.877 \end{bmatrix} \tag{25}$$

$$\delta_{1(1)} = +(\pi - 1)/2 = 1.071 \text{ [rad]}$$

$$\delta_{3(1)} = 0 \qquad .$$

For CMG No. 2 operative

$$\begin{bmatrix} e_{21} \\ e_{22} \\ e_{23} \end{bmatrix} = \begin{bmatrix} 0 \\ 0 \\ -1 \end{bmatrix} \qquad (26)$$

$$\delta_{1(2)} = 0$$

$$\delta_{3(2)} = \pi/2 \text{ [rad]} \quad .$$

For CMG No. 3 operative

$$\begin{bmatrix} e_{31} \\ e_{32} \\ e_{33} \end{bmatrix} = \begin{bmatrix} -0.479 \\ 0 \\ -0.877 \end{bmatrix} \qquad (27)$$

$$\delta_{1(3)} = 0$$

$$\delta_{3(3)} = +(\pi - 0.5) \text{ [rad]} \quad .$$

This window selection insures that no gimbal stops are encountered for the whole range of possible solar elevation angles η_x (-1.265 [rad] to +1.265 [rad]).

TACS CONTROL

The thruster attitude control system (TACS) is used to insure that the CMG angular momentum does not exceed the prescribed "window" and it also insures that the vehicle angular rate about the axis not controlled by the GMG remains within a specified deadband.

The TACS consists of six cold gas thrusters, which are selected and fired individually. The thrusters are mounted on Skylab as shown in Figure 2. The main torque polarities of the thrusters are shown in Table 4. It is also shown in the table that there is a built-in cross-coupling between the vehicle x- and z-axis, and only firing of the appropriate pairs will eliminate this cross-coupling, as much as tolerances and misalignments allow.

The thruster attitude control system fires a minimum impulse bit whenever $|\psi_i| \geq 1$ for any axis [6]. This property is used in Table 5 by allowing only three states for ψ_i : 0 and ± 1.

The thrusters are selected according to Table 5.

For proper initial conditions and for no other than gravity-gradient torques, the cyclic gravity-gradient torques are absorbed by the CMG and the nominal momentum profile of Figure 1 results. The variation of the angular momentum of the CMG along the orbital z-axis (see Figure 3) acts as a disturbance and the gravity-gradient torque provides a restoring torque on the minimum moment-of-inertia axis whenever a z-torque drives it out of the orbital plane by ϕ_{zeo}. The nominal profiles for ϕ_{zeo} and $\dot{\phi}_{zeo}$ of Figures 4 and 5 result if the proper initial conditions have been chosen. The nominal ϕ_{zeo} profile is an unstable limit cycle and will diverge until $\dot{\phi}_{zeo}$ exceeds its deadband and is reduced by a thruster firing (Figs. 6 and 7). The objective of minimum fuel consumption requires that the deadband is wide enough to allow the ideal limit cycle, but still narrow enough such that only one firing is required whenever TACS is actuated, which should reset the initial conditions as close as possible to the ideal case with the hope that there will be several orbits devoid of thruster firings. In other words, the value of the deadband is very critical and will have to be set repeatedly during flight, especially since it is also dependent upon the momentum change due to a minimum impulse bit from the thrusters, as well as disturbance torques and other influences. While a wrong deadband value (either too high or too low) is not disastrous, it does result in an increase of the thruster fuel consumption, and should be corrected as soon as possible.[1]

A constant z-torque results automatically in an average hang-off of the x-axis out of the orbital plane. Several times the presently assumed vent torques can be handled without an increase in the fuel consumption. The deadband, however, has to be adjusted if the torque varies.

---

1. The worst-case fuel consumption of 50 [N-s] per orbit (quoted in the introduction) does not assume worst case for the deadband, but only for the solar elevation angle and the disturbance torques.

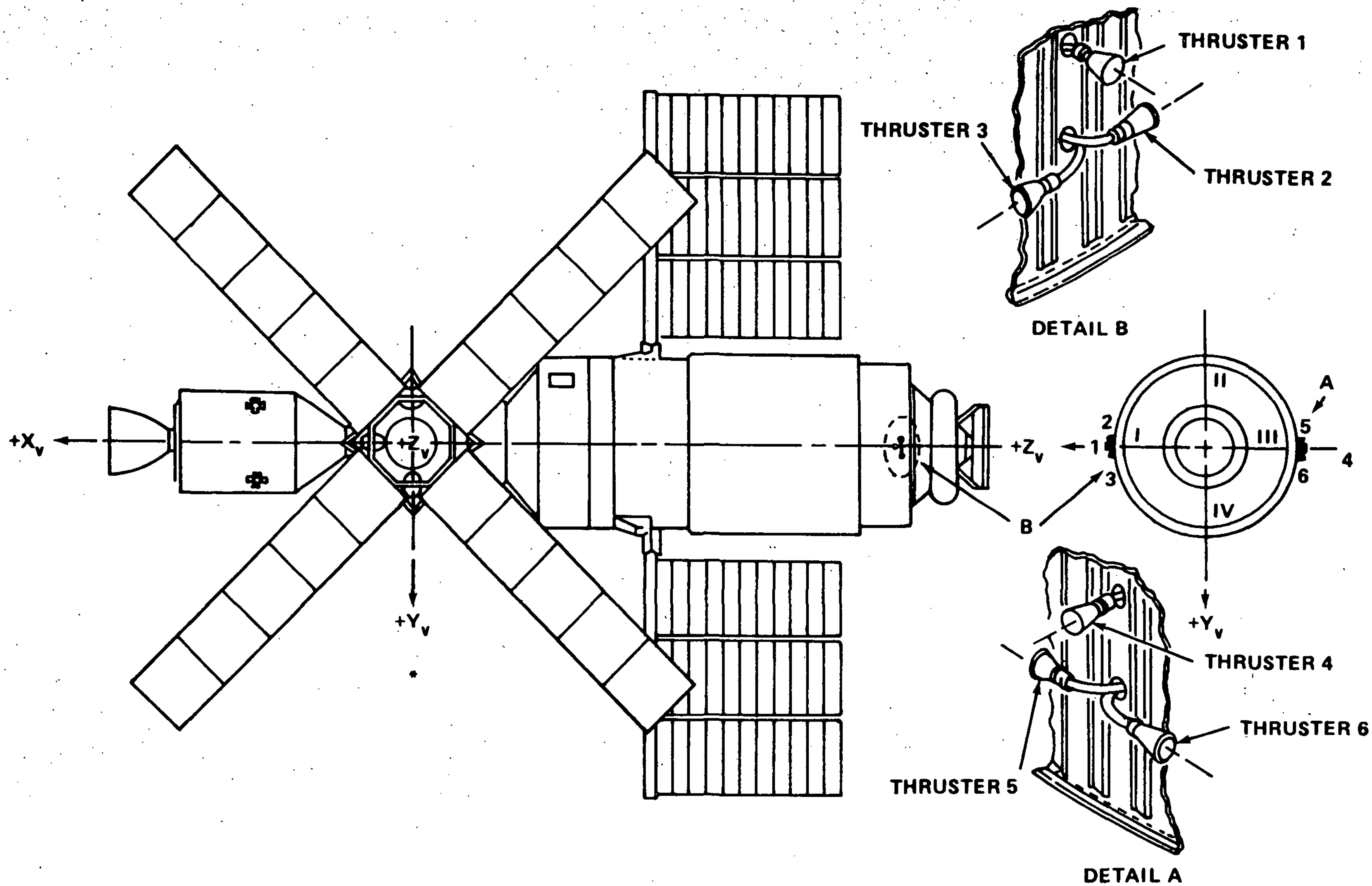

Figure 2. TACS configuration.

TABLE 4. MAIN TORQUE POLARITY

Thruster	x_v-Axis	y_v-Axis	z_v-Axis
1	0	-	0
2	-	0	-
3	+	0	+
4	0	+	0
5	+	0	-
6	-	0	+

TABLE 5. THRUSTER SELECTION

Condition		Selected Thruster
ψ_x	+ 1	2
	0	None
	- 1	3
ψ_y	+ 1	1
	0	None
	- 1	4
ψ_z	+ 1	5
	0	None
	- 1	6

In the following discussion, reference to an x-firing indicates the firing is caused by the momentum exceeding the limits set for H_{xv}, a y-firing is caused by H_{yo} exceeding its limits, and a z-firing is caused by $\dot{\phi}_{zeo}$ exceeding its deadband.

A constant y-torque results in the appropriate change in the desaturation angle ϕ_{yd} and in an increase in the amplitude of the cyclic momentum.

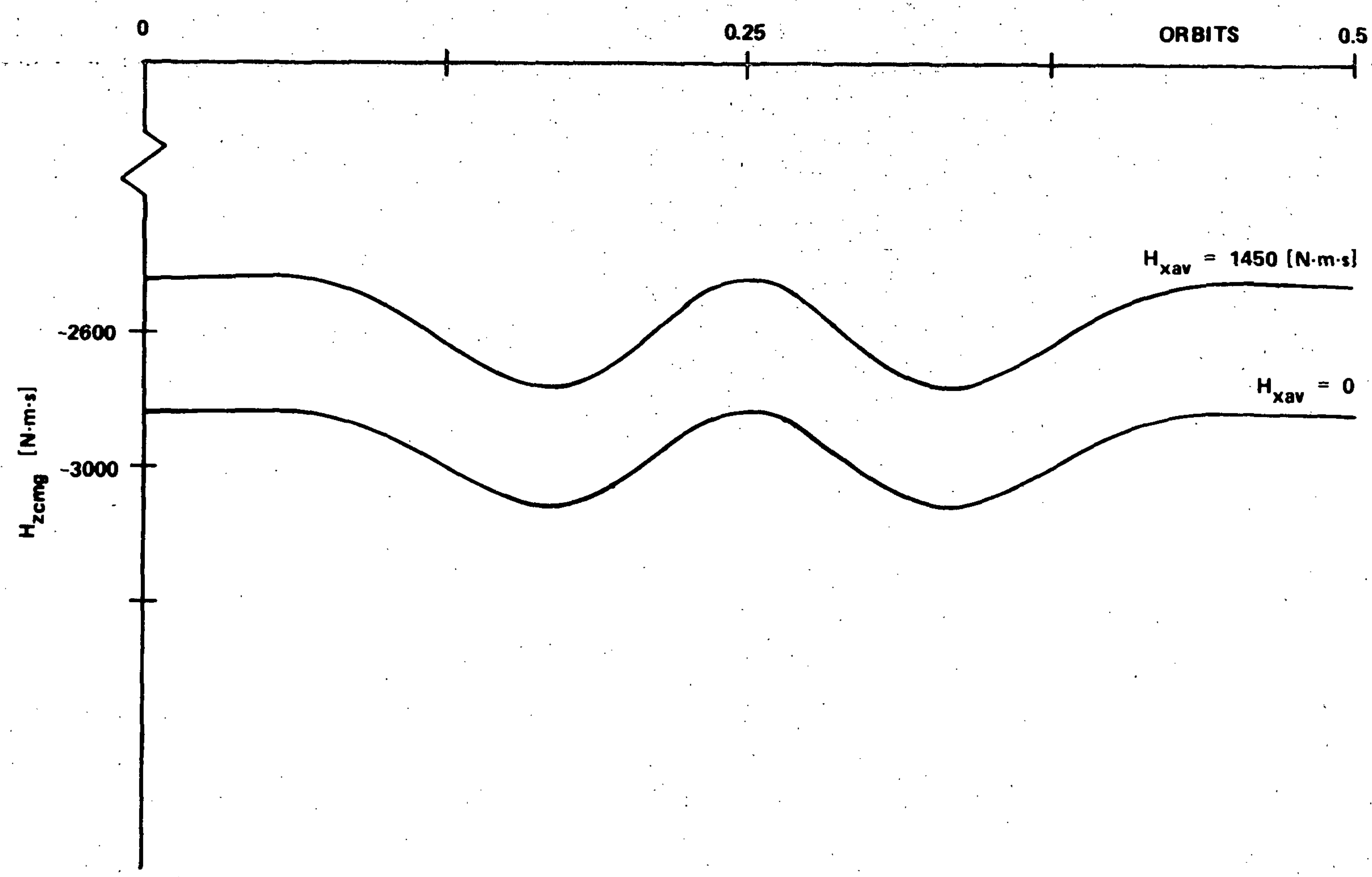

Figure 3. CMG orbital z-momentum component (ideal limit cycle).

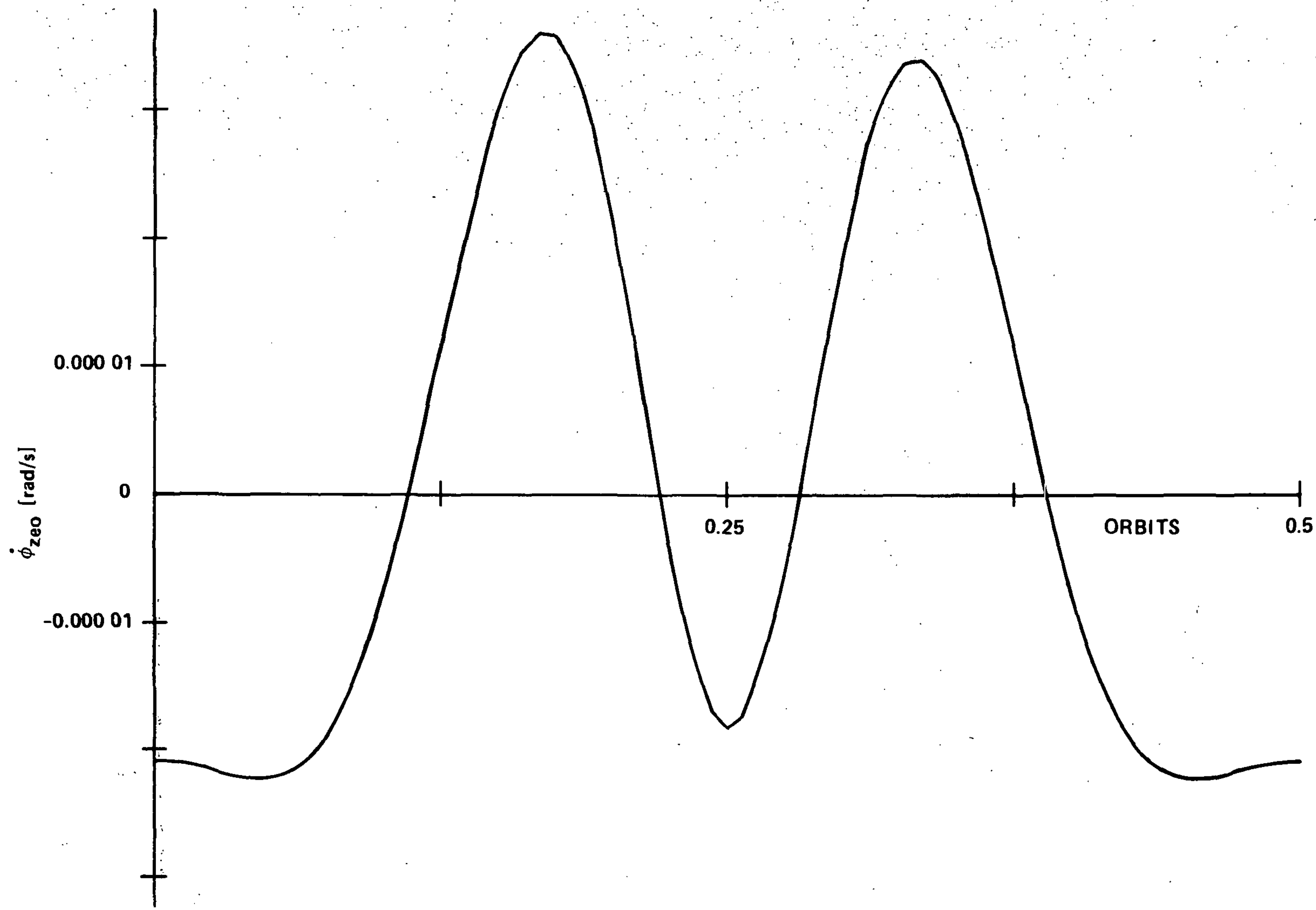

Figure 4. Angular velocity $\dot{\phi}_{zeo}$ (ideal limit cycle).

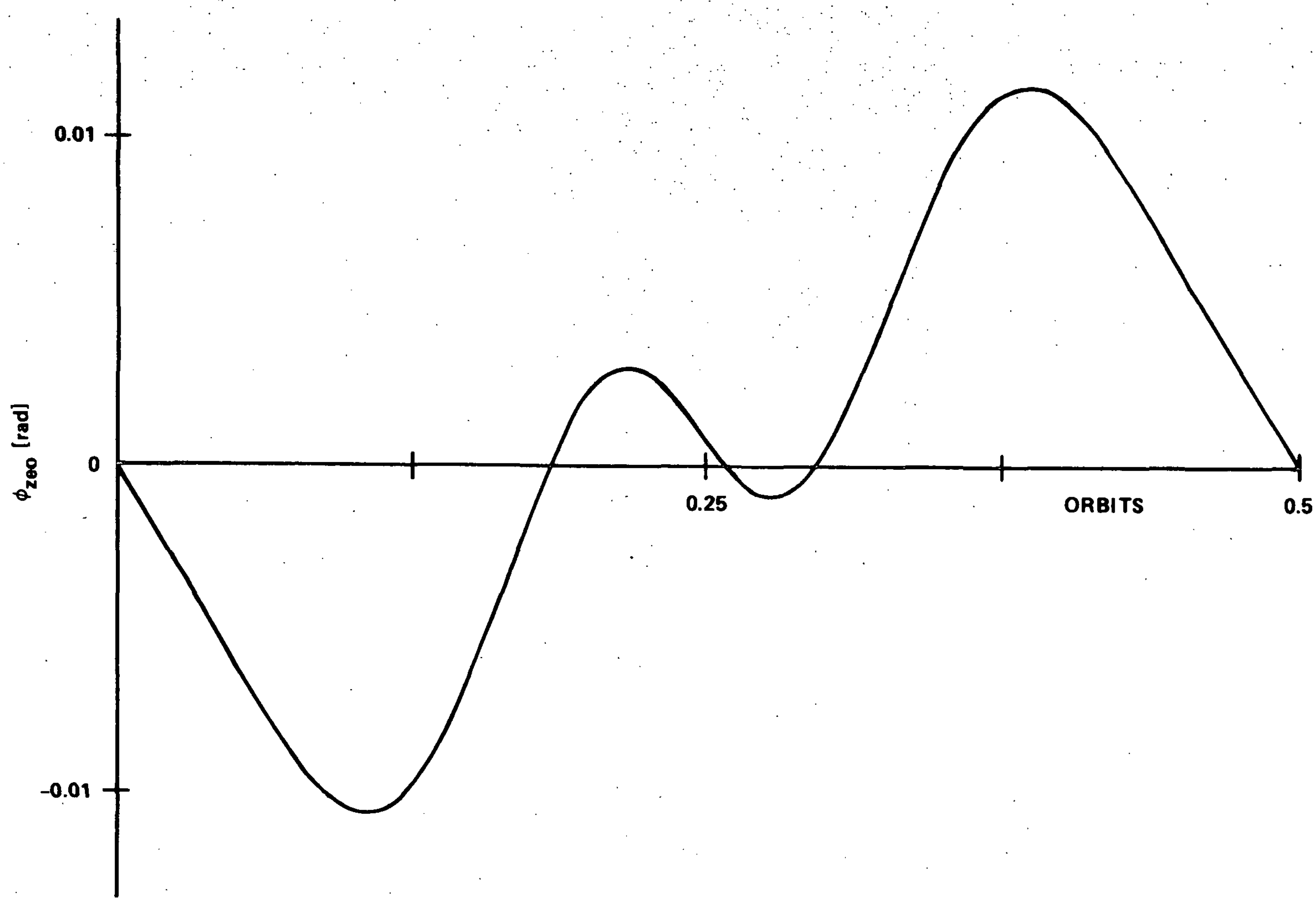

Figure 5. Angle ϕ_{zeo} (ideal limit cycle).

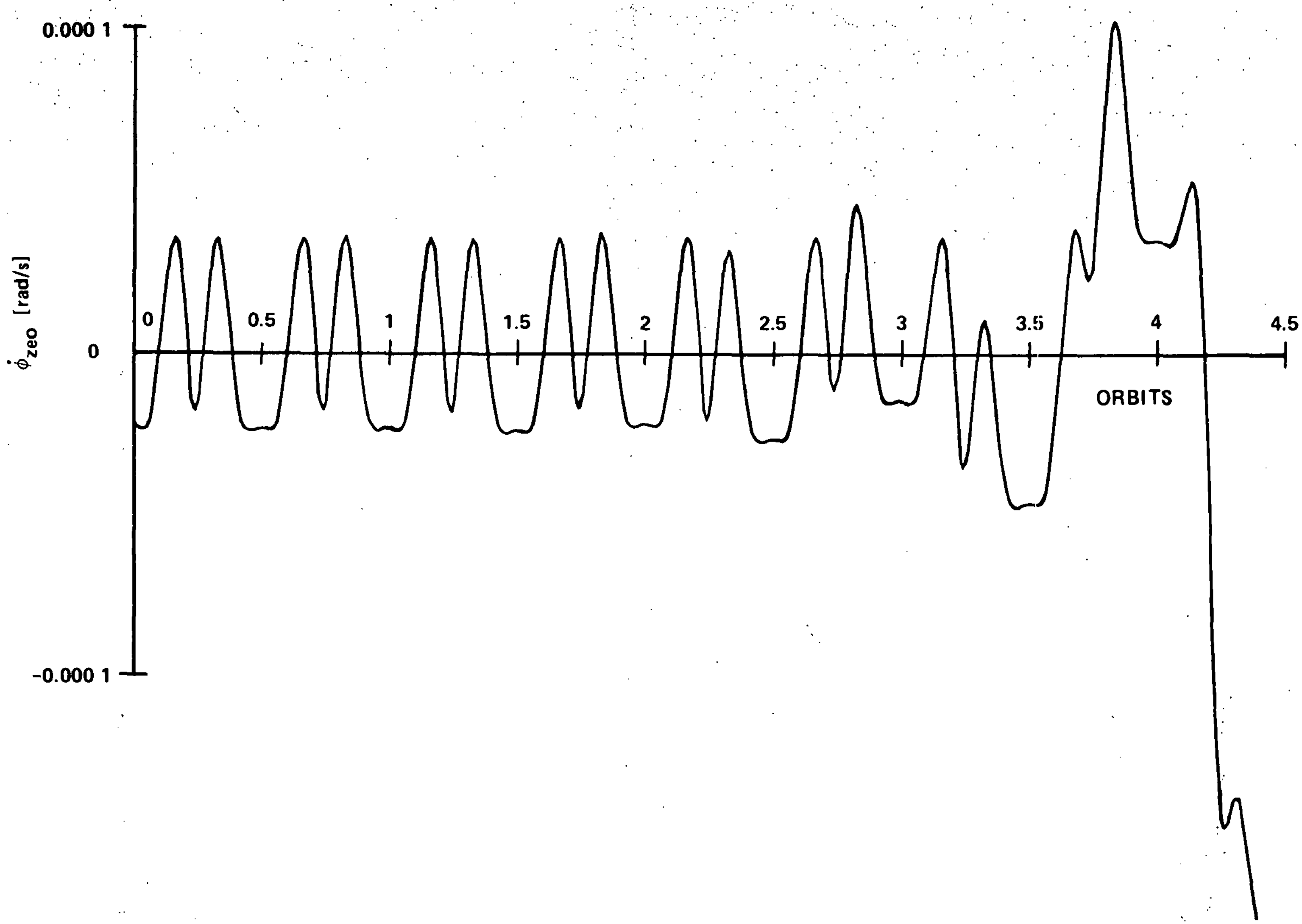

Figure 6. Long term instability of $\dot{\phi}_{zeo}$.

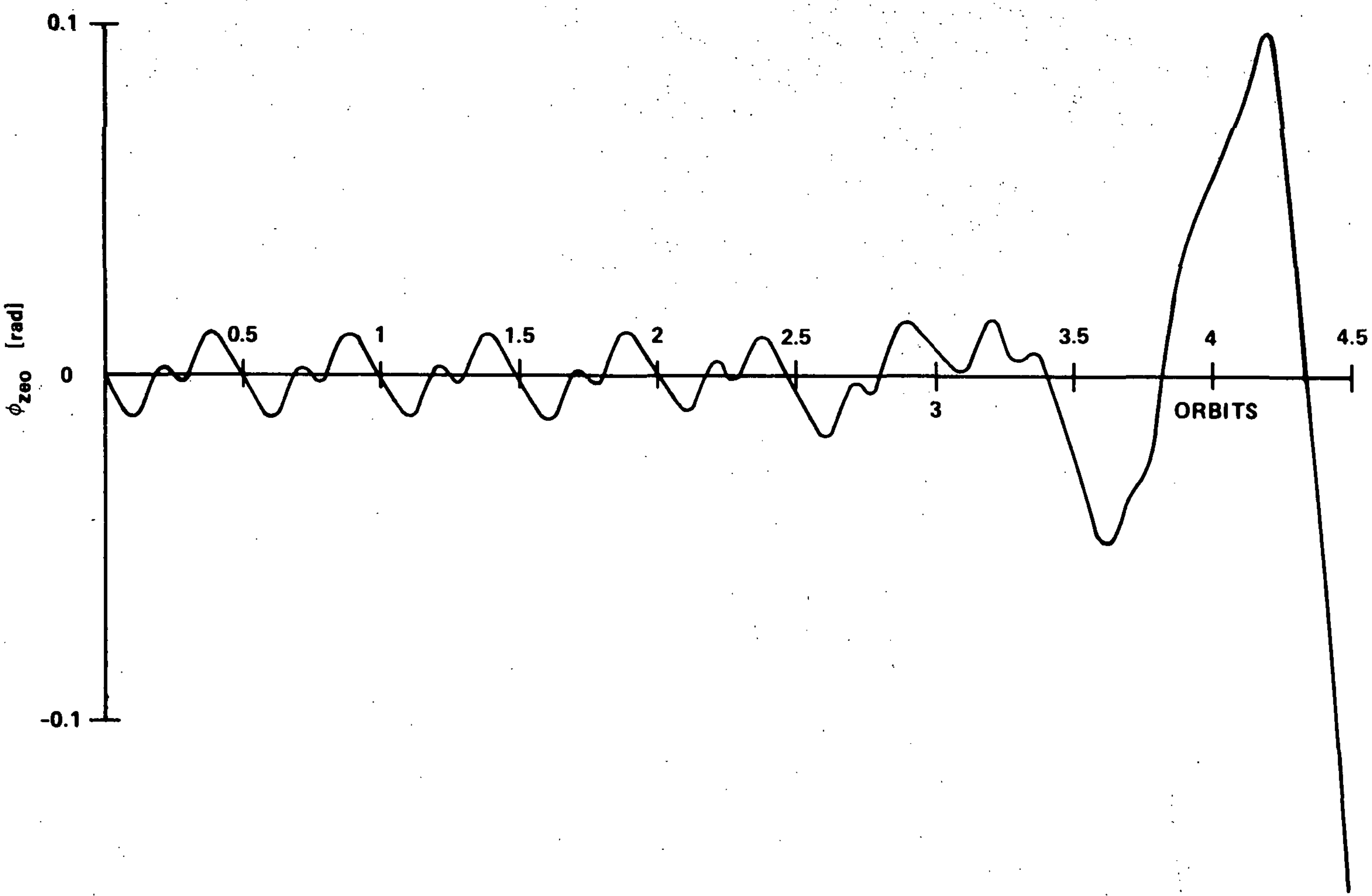

Figure 7. Long term instability of ϕ_{zeo}.

Since the amplitude is bounded, the desaturation angle ϕ_{yd} has to be limited, and any excess momentum has to be desaturated by the thrusters. However, the ϕ_{yd}-limit can desaturate about twice the anticipated disturbance momentum.

A constant x-torque will have to be eliminated entirely by thruster firings. Since the z-limit cycle is very sensitive, any cross-coupling from x-firings would be highly undesirable and therefore pure x-firings will always be in pairs. However, when a thruster is fired on a ψ_z command, it is also utilized to reduce the x-momentum with respect to the nominal x-momentum. Due to the commanded oscillation in the orbital plane, the nominal x-momentum translates into a sinusoidal momentum H_{xb} in vehicle coordinates:

$$H_{xb} = Hs(\phi_{yc} - \phi_{yb}) \tag{28}$$

where ϕ_{yb} is a bias angle that depends upon which of the CMG's is operative ($\phi_{yb} = -0.5$ [rad] for CMG 1; $\phi_{yb} = 0$ for CMG 2; $\phi_{yb} = +0.5$ [rad] for CMG 3).

A y-firing (indicated by $\psi_{yo} \neq 0$) will, through its effect on the CMG orbital z-momentum, also always decrease the magnitude of $\dot{\phi}_{zeo}$. It should, therefore, receive priority over the other firings. If $|\eta_x| > \pi/4$, the appropriate polarity ψ_z is selected instead of ψ_y. A z-firing is not only called for whenever $\dot{\phi}_{zeo}$ exceeds its bounds, but also when it can be clearly established that it has the wrong polarity with respect to the desired limit cycle. Figure 3 in conjunction with Figure 1 shows that $\dot{\phi}_{zeo}$ should be positive for $|H_{yo}|$ less than some lower value H_{yll} and negative for $|H_{yo}|$ above some upper value H_{yul}. The values for these limits depend on the disturbance torques and have to be established during flight. Once the need for a z-firing has been established, it remains to be determined which conbination of ψ_y and ψ_z (which produce momentum changes in vehicle coordinates) is most beneficial in reducing the magnitude of $\dot{\phi}_{zeo}$ while minimizing the cumulative effect of the z-firings on H_{yo}. The reason for the latter is elimination, as much as possible, of cross-coupling into H_{yo}. To do this, five firing combinations are evaluated in terms of their effect on H_{yo} and $\dot{\phi}_{zeo}$. The five combinations are

ψ_y	0	+ 1	- 1	+ 1	- 1
ψ_z	ψ_{zo}	ψ_{zo}	ψ_{zo}	0	0

The following formulas are used (the latter is also in momentum rather than angular velocity):

$$\Delta H = R_x f_t(\Delta t_{mib} + t_{td}) \quad , \tag{29}$$

$$\Delta H' = \Delta H[\max(c\eta_x, |s\eta_x|)] \quad , \tag{30}$$

$$\Delta H_{yo} = \Delta H(c\eta_x\psi_y - s\eta_x\psi_z) \quad , \tag{31}$$

$$\begin{aligned} \Delta H_{zo} &= \Delta H c\phi_{yc}(s\eta_x\psi_y + c\eta_x\psi_z) \\ &\quad + \sqrt{H^2 - H_{xo}^2 - (H_{yo} + \Delta H_{yo})^2} \\ &\quad - \sqrt{H^2 - H_{xo}^2 - H_{yo}^2} \quad . \end{aligned} \tag{32}$$

Equation (29) represents the angular minimum impulse bit for a vehicle y- or z-firing. R_x is the thruster lever arm (a negative value), f_t is the thruster force, Δt_{mib} is the commanded ON-time and t_{td} is a correction factor for thrust decay. $\Delta H'$ gives the nominal ΔH_{zo} for a single engine firing and it is used in equation (33). The difference in the roots of equation

(32) represents the effect of the orbital y-momentum change on $\dot{\phi}_{zeo}$ through the CMG momentum change. Any firing combination which does not produce a ΔH_{zo} with at least half of $\Delta H'$ with the correct polarity will be disregarded. The rest will be evaluated according to their demerits:

$$D = \left| \sum \Delta H_{yoz} + \Delta H_{yo} \right| + K_d \left| \Delta H_{zo} \psi_{zo} - \Delta H' \right| \qquad (33)$$

where $\sum \Delta H_{yoz}$ is the accumulated effect of the z-firings on H_{yo} since the last checkpoint. The first term results in demerits for increasing the effect on H_{yo}, the last term penalizes deviation from the most beneficial single engine firing, and K_d (<1) allows relative weighing of the two. The firing combination with the smallest demerit D is selected.

Simpler firing logic has been investigated, but large cross-coupling was produced between the orbital y- and z-axis, resulting in strong positive feedback at certain η_x angles, so that settling out of ϕ_{yd} was not guaranteed.

A flow chart of the logic with equations is given in Appendix D. To reduce coupling into the desaturation equations, the following quantities have to be updated by the expected value of ΔH_{yo} (= is here a FORTRAN equal):

$$H'_{yo(n-1)} = H'_{yo(n-1)} + \Delta H_{yo} \quad ,$$

$$H_{max} = H_{max} + \Delta H_{yo} \quad ,$$

$$H_{min} = H_{min} + \Delta H_{yo} \quad ,$$

$$\sum \Delta H_{yoz} = \sum \Delta H_{yoz} + \Delta H_{yo} | \psi_{zo} | \quad ,$$

$$\sum \Delta H_{yoy} = \sum \Delta H_{yoy} + \Delta H_{yo} | \psi_{yo} | \quad .$$

DISCUSSION

Long-term drift of the strapdown computation for the attitude reference can be eliminated by slightly modifying the normal Skylab updating method, where the output of the sun sensors is compared with the calculated attitude. Updating is possible whenever the magnitude of the sun sensor output is below 0.1 rad. This occurs three times per orbit (sunrise terminator, noon, and sunset terminator) and lasts for about 460 s (for an amplitude A of 0.2 rad).

Some TACS ONLY attitude control along the lines of References 4 and 5 must be incorporated to be prepared in case the last of the three ATM CMG's also fails.

APPENDIX A

DEFINITIONS OF SKYLAB COORDINATE SYSTEMS (CS's)

Only the coordinate systems (CS's) needed for this memorandum are defined. All CS's are right-handed and orthogonal. All angles are defined mathematically positive.

Symbol	Transformation Matrix	Definition
x_o, y_o, z_o	N/A	Basic orbital CS; z_o toward ascending node; y_o toward orbital north.
x_r, y_r, z_r	$X_r = [\eta_x][\eta_y]X_o$	Reference CS; z_r toward sun; x_r in the orbital plane; y_r in northern orbital hemisphere.
x_{or}, y_{or}, z_{or}	$X_{or} = [\eta_x]^T X_r$	Orbital references CS; z_{or} along projection of z_r into orbital plane; y_{or} toward orbital north.
x_v, y_v, z_v	$X_v = [q_{va}]X_r$	Vehicle geometric CS. Also the attitude control system CS. $[q_{va}]$ indicates the attitude deviation from x_r (due to error or commands). This CS is also assumed to be the principal CS for the development of the equations in this report.

Symbol	Transformation Matrix	Definition
x_{vc}, y_{vc}, z_{vc}	$X_{vc} = [\eta_x][\phi_{zeo}][\phi_{yc}]X_{or}$	Commanded vehicle CS. η_x in this transformation is only numerically equal to the solar elevation angle, but physically it is a different angle.
x_d, y_d, z_d	$X_d = [\eta_t]X_{or}$	Disturbance CS; z_d toward center of earth; y_d toward orbital north ($\eta_t = 0$ indicates orbital midnight; η_t is a y angle).

APPENDIX B

DESATURATION EFFECTIVENESS

The gravitational orbital y-torque is [refer to equation (4)]

$$T_{yo} = -\frac{3}{2}\Omega^2 \Delta I s2[\eta_t - As2(\eta_t - \phi_{yd})]$$

where ϕ_{yd} is the desaturation angle. The y-momentum after half an orbit is (H_{yoic} is the initial momentum)

$$H_{yo} = H_{yoic} + \int_0^{T_{orb}/2} T_{yo} dt$$

or

$$H_{yo} - H_{yoic} = -\frac{3}{2}\Omega \Delta I \int_0^{\pi} s2[\eta_t - As2(\eta_t - \phi_{yd})] d\eta_t \quad .$$

The integral is broken into two parts

$$H_{yo} - H_{yoic} = -\frac{3}{2}\Omega \Delta I \, (I_1 + I_2)$$

with

$$I_1 = \int_0^{\pi/2} s2[\eta_t - As2(\eta_t - \phi_{yd})] d\eta_t$$

$$I_2 = \int_{\pi/2}^{\pi} s2[\eta_t - As2(\eta_t - \phi_{yd})] d\eta_t \quad .$$

A substitution of $\alpha = \pi - \eta_t$ into I_2 yields

$$I_2 = -\int_0^{\pi/2} s2[\alpha - As2(\alpha + \phi_{yd})]d\alpha \quad .$$

Since α is only a dummy integration variable, any variable can be substituted. The author elected to substitute η_t and get for the sum of the two integrals

$$(H_y - H_{yo})/(-3\Omega\Delta I/2) = \int_0^{\pi/2} F(\eta_t)d\eta_t$$

with

$$F(\eta_t) = s2[\eta_t - As2(\eta_t - \phi_{yd})] - s2[\eta_t - As2(\eta_t + \phi_{yd})] \quad .$$

This expression shows that for $\phi_{yd} = 0$ the integral is zero. Further development of $F(\eta_t)$ yields

$$F(\eta_t) = s2\{\eta_t - A[s2\eta_t c2\phi_{yd} - c2\eta_t s2\phi_{yd}]\} - s2\{\eta_t - A[s2\eta_t c2\phi_{yd} + c2\eta_t s2\phi_{yd}]\}$$

$$= s2(\eta_t - As2\eta_t c2\phi_{yd})c(2Ac2\eta_t s2\phi_{yd}) + c2(\eta_t - As2\eta_t c2\phi_{yd})s(2Ac2\eta_t s2\phi_{yd})$$

$$-s2(\eta_t - As2\eta_t c2\phi_{yd})c(2Ac2\eta_t s2\phi_{yd}) + c2(\eta_t - As2\eta_t c2\phi_{yd})s(2Ac2\eta_t s2\phi_{yd})$$

$$= 2c2(\eta_t - As2\eta_t c2\phi_{yd})s(2Ac2\eta_t s2\phi_{yd})$$

$$= 2[c2\eta_t c(2As2\eta_t c2\phi_{yd})s(2Ac2\eta_t s2\phi_{yd})$$

$$+ s2\eta_t s(2As2\eta_t c2\phi_{yd})s(2Ac2\eta_t s2\phi_{yd})]$$

The last tern of $F(\eta_t)$ is antisymmetric with respect to $\eta_t = \pi/4$ and does not result in a contribution when the integration is performed from $\eta_t = 0$ to $\eta_t = \pi/2$. The final result is

$$H_{yo} - H_{yoic} = -6\Omega\Delta I \int_0^{\pi/4} c2\eta_t c(K_c s2\eta_t) s(K_s c2\eta_t) d\eta_t$$

with

$$K_c = 2Ac2\phi_{yd}$$

$$K_s = 2As2\phi_{yd}$$

where the integration is only from zero to $\pi/4$ because of the symmetry with respect to $\pi/4$ and the result is doubled. The effectiveness of ϕ_{yd} had to be established by numerical integration, but small angle approximation shows that the accumulated momentum is proportional to ϕ_{yd} :

$$H_{yo} - H_{yoic} = G_{yd}\phi_{yd}$$

with

$$G_{yd} = -24\Omega\Delta IA \int_0^{\pi/4} c^2(2\eta_t)c(2As2\eta_t)d\eta_t \qquad .$$

APPENDIX C

LOGIC FOR ORBITAL y-MOMENTUM DESATURATION

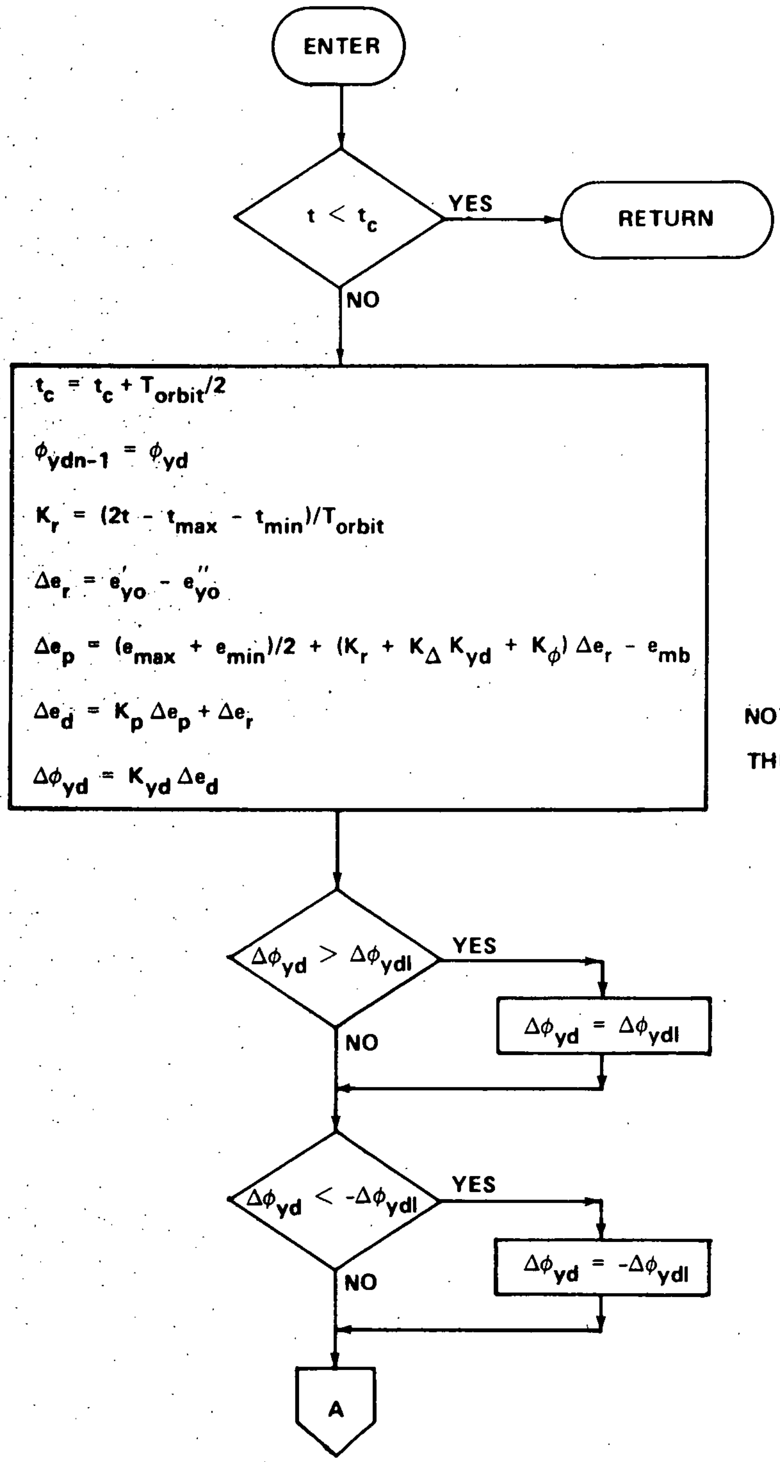

NOTE: THE FIRST TIME THROUGH SET $\Delta\phi_{yd} = 0$.

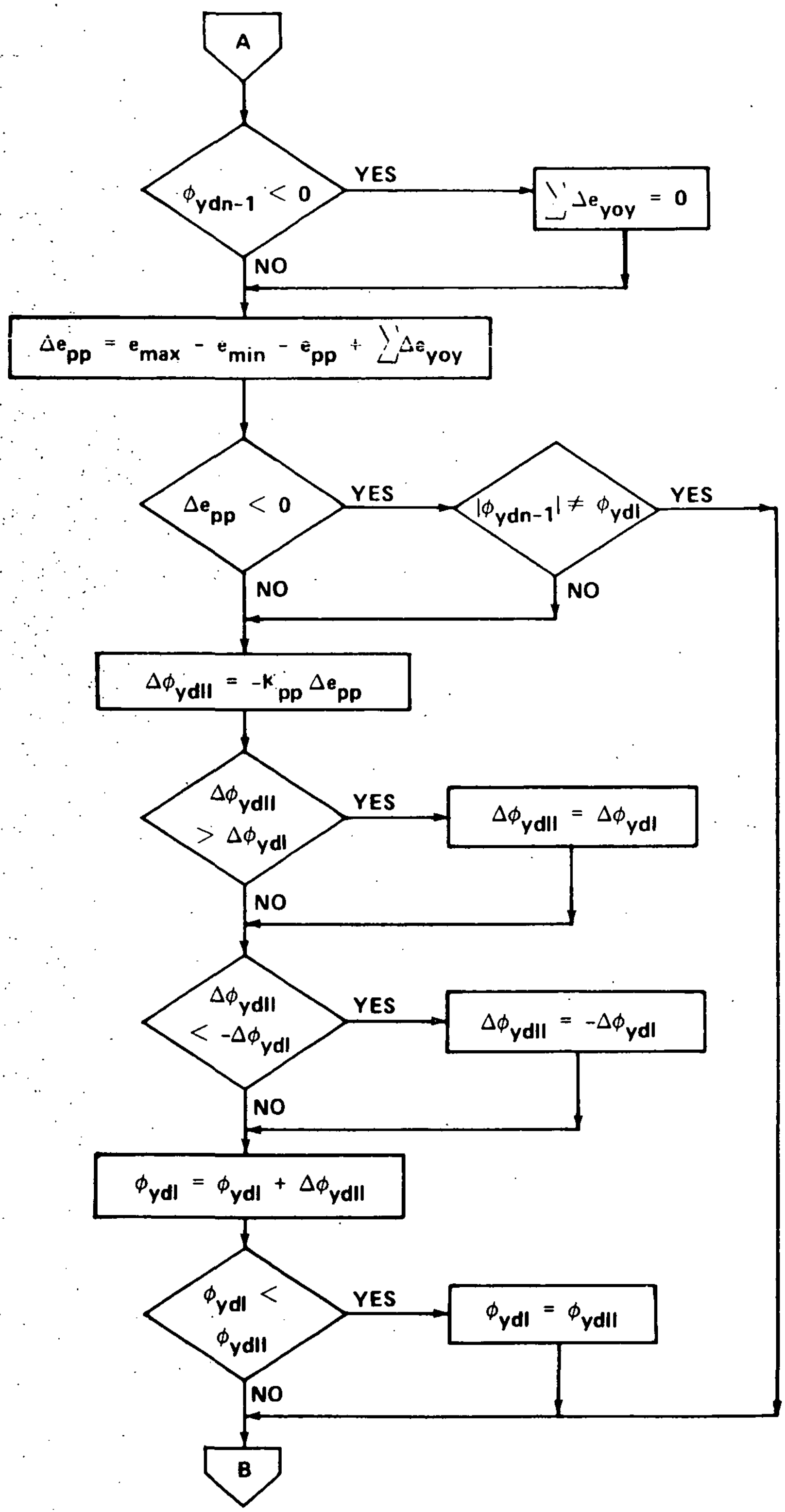
A
$\phi_{ydn-1} < 0$
YES
$\sum \Delta e_{yoy} = 0$
NO
$\Delta e_{pp} = e_{max} - e_{min} - e_{pp} + \sum \Delta e_{yoy}$
$\Delta e_{pp} < 0$
YES
$|\phi_{ydn-1}| \neq \phi_{ydl}$
YES
NO
NO
$\Delta\phi_{ydll} = -K_{pp}\,\Delta e_{pp}$
$\Delta\phi_{ydll} > \Delta\phi_{ydl}$
YES
$\Delta\phi_{ydll} = \Delta\phi_{ydl}$
NO
$\Delta\phi_{ydll} < -\Delta\phi_{ydl}$
YES
$\Delta\phi_{ydll} = -\Delta\phi_{ydl}$
NO
$\phi_{ydl} = \phi_{ydl} + \Delta\phi_{ydll}$
$\phi_{ydl} < \phi_{ydll}$
YES
$\phi_{ydl} = \phi_{ydll}$
NO
B

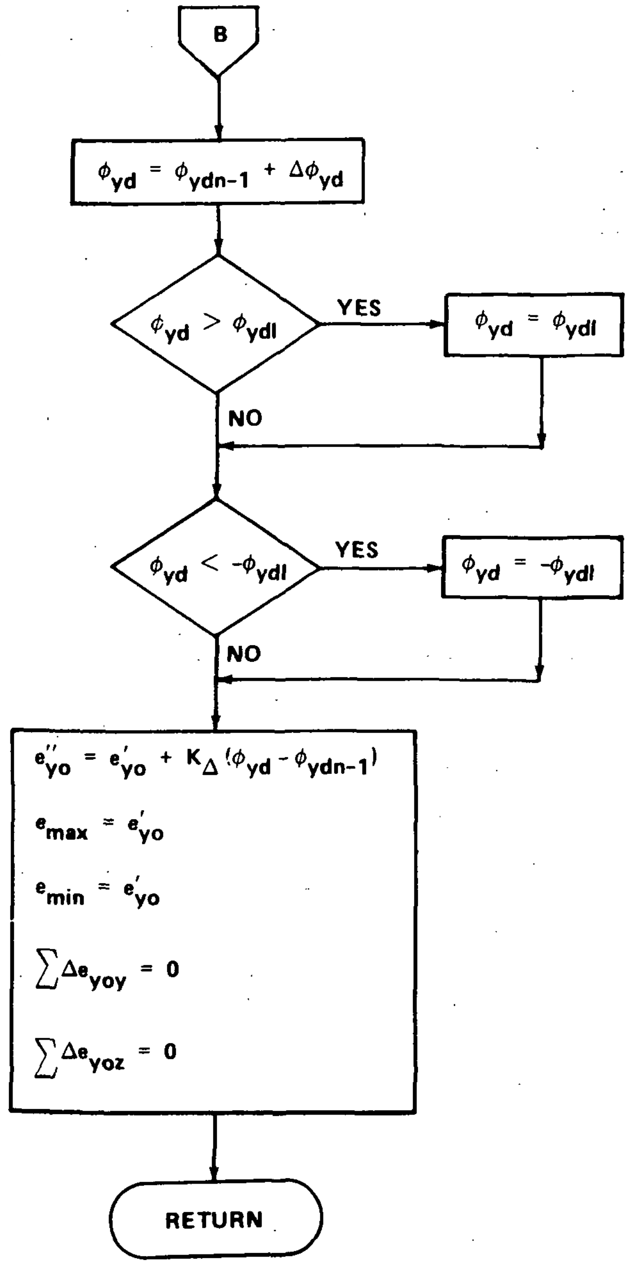
B
$\phi_{yd} = \phi_{ydn-1} + \Delta\phi_{yd}$
$\phi_{yd} > \phi_{ydl}$
YES
$\phi_{yd} = \phi_{ydl}$
NO
$\phi_{yd} < -\phi_{ydl}$
YES
$\phi_{yd} = -\phi_{ydl}$
NO
$e''_{yo} = e'_{yo} + K_\Delta(\phi_{yd} - \phi_{ydn-1})$
$e_{max} = e'_{yo}$
$e_{min} = e'_{yo}$
$\sum \Delta e_{yoy} = 0$
$\sum \Delta e_{yoz} = 0$
RETURN

APPENDIX D

EXTREMA OF H_{yo} AND TACS FIRING LOGIC

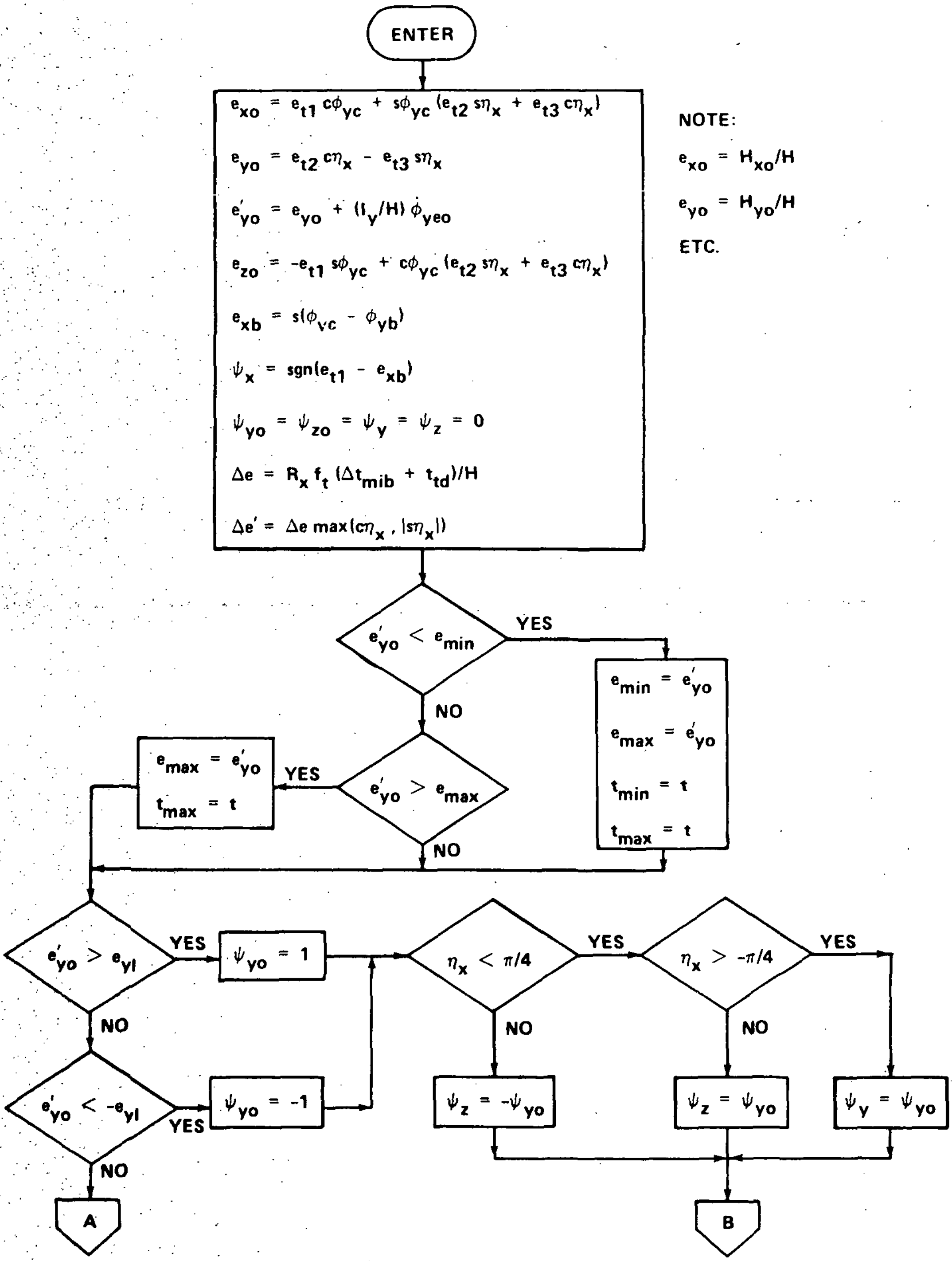

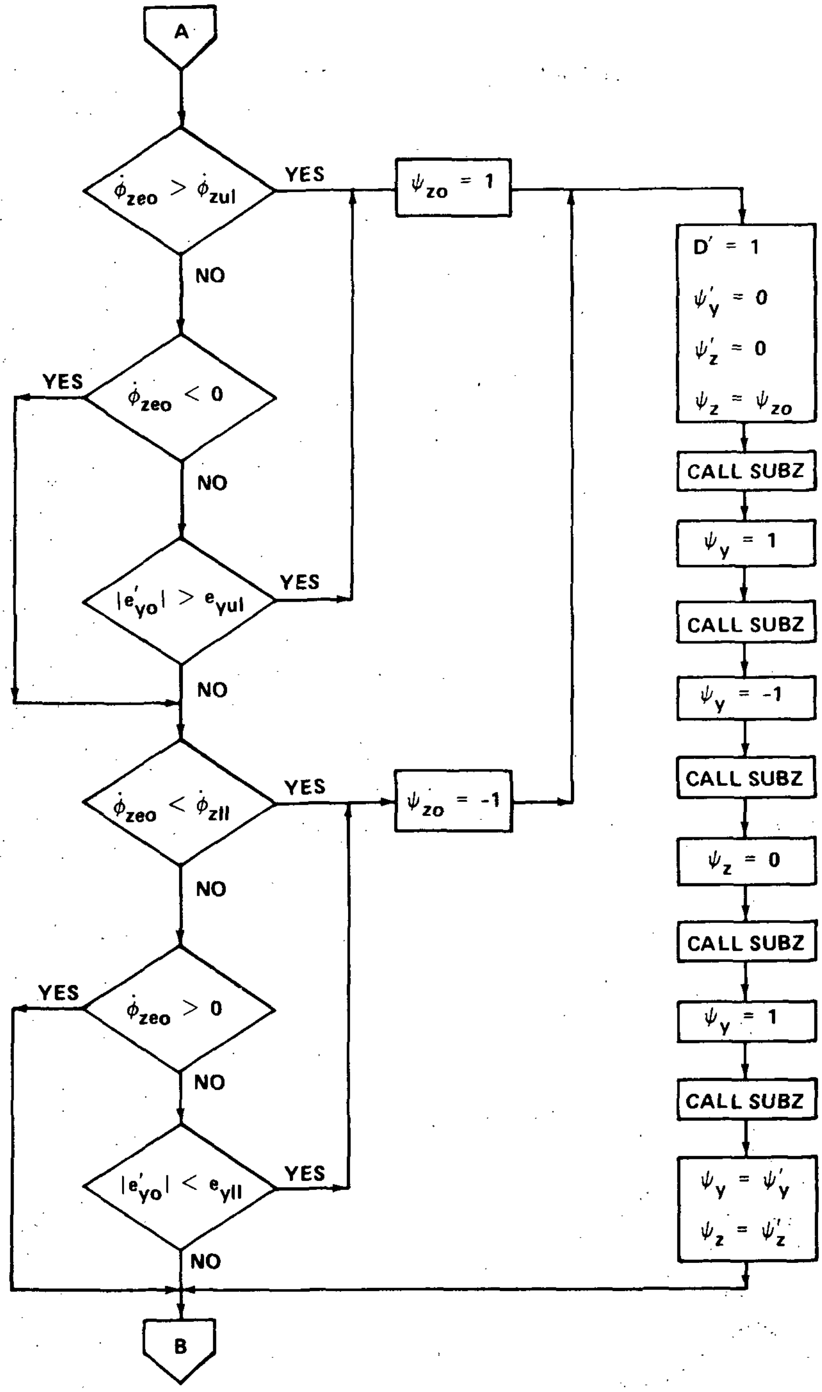
A
$\dot{\phi}_{zeo} > \dot{\phi}_{zul}$
YES
NO
$\psi_{zo} = 1$
$D' = 1$
$\psi'_y = 0$
$\psi'_z = 0$
$\psi_z = \psi_{zo}$
$\dot{\phi}_{zeo} < 0$
YES
NO
CALL SUBZ
$\psi_y = 1$
$|e'_{yo}| > e_{yul}$
YES
NO
CALL SUBZ
$\psi_y = -1$
$\dot{\phi}_{zeo} < \dot{\phi}_{zll}$
YES
NO
$\psi_{zo} = -1$
CALL SUBZ
$\psi_z = 0$
$\dot{\phi}_{zeo} > 0$
YES
NO
CALL SUBZ
$\psi_y = 1$
CALL SUBZ
$|e'_{yo}| < e_{yll}$
YES
NO
$\psi_y = \psi'_y$
$\psi_z = \psi'_z$
B

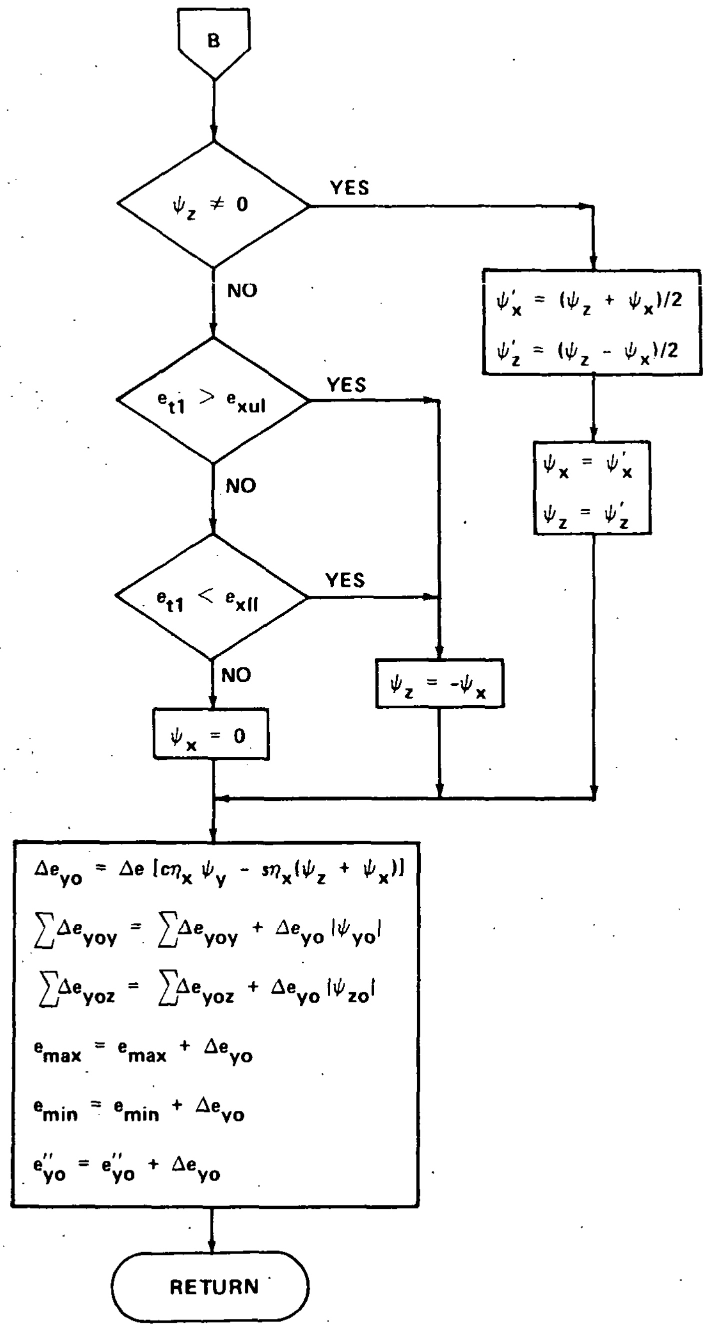

B
$\psi_z \neq 0$
YES
NO
$\psi'_x = (\psi_z + \psi_x)/2$
$\psi'_z = (\psi_z - \psi_x)/2$
$e_{t1} > e_{xul}$
YES
NO
$\psi_x = \psi'_x$
$\psi_z = \psi'_z$
$e_{t1} < e_{xll}$
YES
NO
$\psi_z = -\psi_x$
$\psi_x = 0$
$\Delta e_{yo} = \Delta e\,[c\eta_x\,\psi_y - s\eta_x(\psi_z + \psi_x)]$
$\sum\Delta e_{yoy} = \sum\Delta e_{yoy} + \Delta e_{yo}\,|\psi_{yo}|$
$\sum\Delta e_{yoz} = \sum\Delta e_{yoz} + \Delta e_{yo}\,|\psi_{zo}|$
$e_{max} = e_{max} + \Delta e_{yo}$
$e_{min} = e_{min} + \Delta e_{yo}$
$e''_{yo} = e''_{yo} + \Delta e_{yo}$
RETURN

Subroutine SUBZ

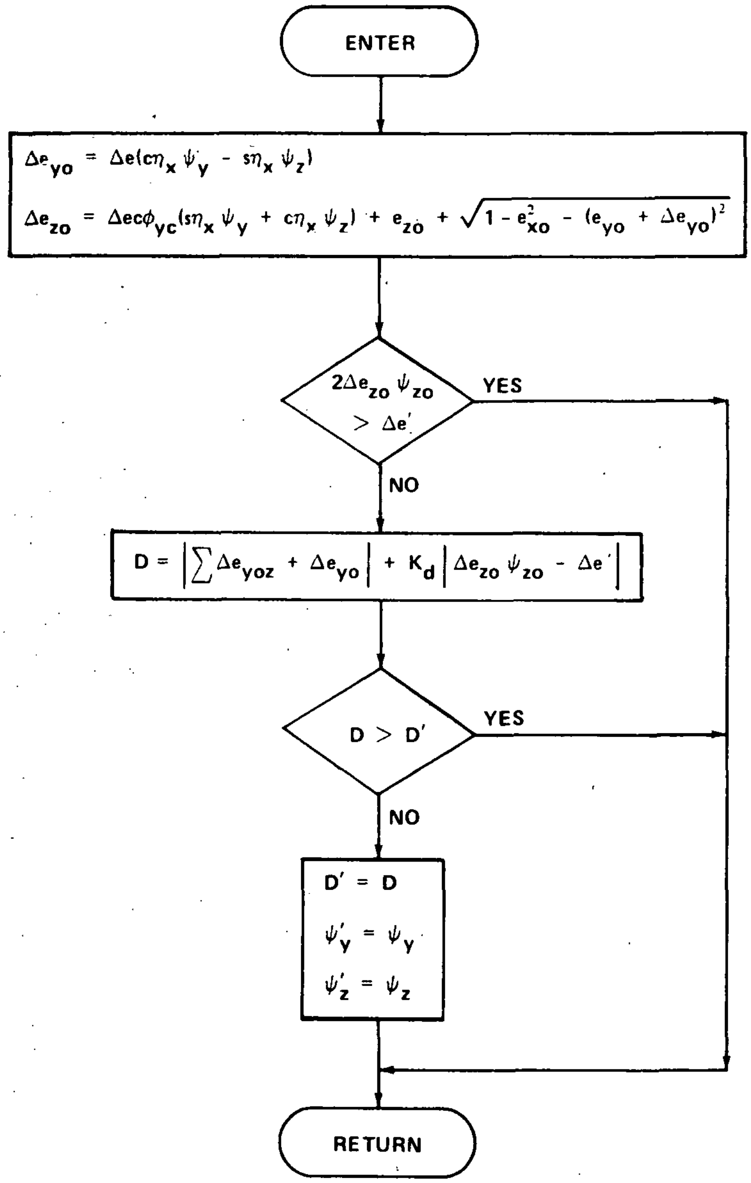

REFERENCES

1. Chubb, W. B. and Seltzer, S. M.: Skylab Attitude Pointing Control System. NASA TN D-6068, October 1970.

2. Kennel, H. F.: A Control Law for Double-Gimbaled Control Moment Gyros Used for Space Vehicle Attitude Control. NASA TM X-64536, August 7, 1970.

3. Kennel, H. F.: Angular Momentum Desaturation for Skylab Using Gravity Gradient Torques. NASA TM X-64628, December 7, 1971.

4. Elrod, B. D.: Comparison of Impulse Requirements for Skylab Attitude Control with Exact and Approximate Quasi-Inertial Steering. Bellcomm, TM-71-1022-6, December 30, 1971.

5. Elrod, B. D.: The Quasi-Inertial and Wide-Deadband Modes as Backup Attitude Options for the Skylab Mission. Bellcomm, TM-71-1022-3, June 19, 1971.

6. IBM Federal Systems Division: Apollo Telescope Mount Digital Computer Program Definition Document. Report No. 70-207-0002, NASA Contract NAS8-20899, Marshall Space Flight Center, Alabama, August 17, 1972.

APPROVAL

NASA TM X-64746

SKYLAB ATTITUDE CONTROL AND ANGULAR MOMENTUM DESATURATION WITH ONE DOUBLE-GIMBALED CONTROL MOMENT GYRO

By Hans F. Kennel

The information in this report has been reviewed for security classification. Review of any information concerning Department of Defense or Atomic Energy Commission programs has been made by the MSFC Security Classification Officer. This report, in its entirety, has been determined to be unclassified.

This document has also been reviewed and approved for technical accuracy.

Hans H. Hosenthien

HANS H. HOSENTHIEN
Chief, R&D Analysis Office

F. B. Moore

F. B. MOORE
Director, Astrionics Laboratory